LASER APPLICATIONS AND OTHER TOPICS IN QUANTUM ELECTRONICS

PACS numbers: 07.85.Fv; 41.50.+h
DOI: 10.1070/QE2000v030n05ABEH001736

Broadband x-ray optical elements based on aperiodic multilayer structures

N N Kolachevskiĭ, A S Pirozhkov, E N Ragozin

Abstract. An investigation was made of the potentialities of aperiodic multilayer structures (AMSs) optimised to obtain a preassigned reflection spectrum in the x-ray range ($\lambda < 300$ Å) and also starting from other criteria. It was found that among the multitude of realisations of AMSs there exist those which are superior to the regular structure in width of the operating range, integral reflectivity, and peak reflectivity. New types of x-ray optical elements are proposed on a basis of AMSs. AMSs were derived which possess a constant normal-incidence reflectivity R at normal incidence throughout the 130 – 190 Å ($R = 24\%$), 130 – 300 Å ($R = 15\%$), etc., ranges. We found AMSs which possess a high polarising power (polarisance) and a constant R in a broad wavelength range for a fixed angle of incidence. AMSs possessing several isolated reflection peaks which are not Bragg peaks of one another, were calculated. AMSs intended for operation in the hard x-ray range at grazing incidence of radiation were optimised. The technique elaborated in our work was demonstrated to be efficient for optimising AMSs with a very large ($\sim 10^3$) number of layers.

1. Introduction

The use of multilayer mirrors (MMs) for the reflection of soft x-ray (SXR) radiation ($\lambda \leqslant 300$ Å) was proposed more than 20 years ago [1, 2]. During these decades, the technology for producing efficient multilayer mirrors was elaborated, and MMs themselves now make up an integral part of laboratory and astrophysical experiments. In the 20 – 300 Å range, MMs are used at normal and oblique incidence of radiation. At small grazing angles, MMs can efficiently reflect hard x-ray radiation [3].

We provide some examples of applications of multilayer optics. First, concave MMs are employed to focus x-ray laser and synchrotron radiation beams, the radiation of laser-produced plasma and of other laboratory sources. Objectives comprising two or more MMs are used in x-ray microscopy, microanalysis, and EUV projection lithography systems. A Mach – Zehnder interferometer with multilayer beamsplitters was realised in the $\lambda = 155$ Å range (the wavelength of an x-ray laser on Ne-like Y xxx) [4].

N N Kolachevskiĭ, A S Pirozhkov, E N Ragozin P N Lebedev Physics Institute, Russian Academy of Sciences, Leninskiĭ prospekt 53, 117924 Moscow, Russia; e-mail: ragozin@sci.lebedev.ru

Received 6 December 1999
Kvantovaya Elektronika **30** (5) 428 – 434 (2000)
Translated by E N Ragozin, edited by M N Sapozhnikov

Plane MMs at oblique incidence are used as polarisers of x-ray beams [5, 6]. In astronomy, MMs are used in the design of x-ray telescopes for obtaining images of the Sun and other sources. In combination with absorption filters, plane MMs at oblique incidence (including grazing incidence) serve as reflection filters in x-ray spectrometers for measuring the intensity of radiation of high-temperature plasmas (tokamak, laser-produced plasma) with a relatively poor spectral resolution ($\lambda/\delta\lambda \leqslant 10^2$) [7].

Recently, a start was made on the use of MMs in dispersion spectroscopy to obtain spectra of laser-produced plasmas with high spectral and spatial resolution [8, 9] and to record monochromatic spectral images of the Sun [10]. In combination with a dispersive element (large-aperture transmission or reflection diffraction grating), focusing normal-incidence MMs allowed us to implement spectrometers which offered stigmatism, high resolution (10^4 and over), and high throughput simultaneously – a combination of properties previously inherent only in the instruments of the visible and near-UV range. The operating range of these spectrometers is limited by the resonance reflection band of the MMs involved.

However, there is also demand for panoramic spectrometers with a sufficiently broad operating range (e.g., with $\Delta\lambda/\lambda \sim 0.5 - 1$). One of the possibilities involves using a focusing MM with a strong gradient of the multilayer structure period across the aperture. In this way it became possible to construct a stigmatic spectrograph for the 110 – 300 Å range [11]. A radically different approach involves the search for and the synthesis of multilayer structures possessing sufficiently broad reflection bands. We are evidently dealing with irregular (aperiodic) structures since the optimisation of a periodic structure is reduced to variation of the γ parameter (see below) and retains the resonance nature of reflection.

Modern MMs constitute nanostructures of alternating layers of two different materials (A/B) deposited on plane or figured substrates with a high surface polish. An in-depth layer-thickness regularity of about 1 Å can be attained in the course of structure deposition. The spectral reflectivity profile $R(\lambda)$ inherent in such a regular structure takes the form of a resonance curve that peaks at wavelength $\lambda_{\max}$ defined by the known Bragg equation

$$m\lambda_{\max} \approx 2nd\cos\theta \ ,$$

where $d = d_A + d_B$ is the structure period; n is the refractive index averaged over the period; θ is the angle of incidence with respect to the normal; and m is the order of reflection. The resonance peak width $\Delta\lambda_{1/2}$ is determined by the effective number of interfering rays, which depend on the absorption coefficient at the wavelength involved and, to an extent, on the ratio between the thickness of one of the

layers (usually the strongly absorbing material is implied) and the period $\gamma = d_A/d$. The number of layers may range from ~ 10 to hundreds, and the relative peak width $\Delta\lambda_{1/2}/\lambda_{max}$ from 0.1 in the 300 Å range to 0.01 in the short-wavelength domain.

It is pertinent to note that there has already commenced a discussion in the literature concerning the potentialities of aperiodic multilayer structures (AMSs), primarily from the viewpoint of maximising the integral reflectivity $\mathfrak{J}$ [12–15]. The problem of an MM capable of reflecting SXR radiation at two wavelengths was considered in Ref. [16]. In the above-cited paper [3], Joensen et al. reported the synthesis of a W/Si MM intended for the reflection of x-ray radiation with photon energies up to 70 keV (0.18 Å) at a grazing angle of incidence $\theta = 3$ mrad. Its period decreased monotonically with depth (the concept of a so-called supermirror). An analytical approach was proposed for calculating AMSs with a preassigned $R(\lambda)$ profile in the hard x-ray range [17].

The general formulation of the problem involves the quest for multilayer structures possessing some attractive, preassigned characteristics (e.g., a specific spectral reflectivity profile, high polarisance, etc.). The primary objective of this work was to search for AMSs with a broad, as far as possible, reflection band to be used in dispersion spectroscopy. To this end, a numerical approach was elaborated allowing optimisation of a multilayer structure as regards to various criteria. The numerical technique described below has proven to be efficient in the optimisation of AMSs intended for operation over the entire x-ray range ($\lambda < 300$ Å) for different angles of radiation incidence, including small (grazing) angles of incidence. In this case, the number of AMS layers may be quite large ($\sim 10^3$).

2. Numerical technique

Considering a multilayer structure $\{l_j\}$, $j = 1, \ldots, N$, we shall imply N alternating layers of two different materials deposited on a perfectly smooth substrate of a certain material, which is most often adopted only from the viewpoint of fabrication technology. The interlayer roughness and the existence of transition layers are disregarded at this stage. The layer numbering proceeds inwards, towards the substrate; odd and even layers are formed by different materi-als characterised by complex dielectric constants $\varepsilon_{A,B} = n^2_{A,B} = 1 - \delta_{A,B} + i\beta_{A,B}$. The optical constants δ_A, β_A and δ_B, β_B of the materials are related to the atomic scattering factors $f = f_1 + if_2$ by the formula

$$\begin{pmatrix}\delta\\ \beta\end{pmatrix} = \frac{r_0}{\pi}\lambda^2 N_a \begin{pmatrix}f_1\\ f_2\end{pmatrix}, \tag{1}$$

where $r_0 = e^2/m_e c^2$ is the classical electron radius and N_a is the atom density. Another form of this formula may be convenient to use:

$$\begin{pmatrix}\delta\\ \beta\end{pmatrix} \approx 0.54 \times 10^{-5}\frac{\rho}{\mu}\lambda^2 \begin{pmatrix}f_1\\ f_2\end{pmatrix},$$

where λ is expressed in angstroms, the density of the material ρ in grams per cubic centimetre, and the atomic weight μ in atomic mass units. When the material consists of atoms of several sorts, a more general expression applies:

$$\begin{pmatrix}\delta\\ \beta\end{pmatrix} \approx 0.54 \times 10^{-5}\frac{\rho}{\sum \alpha_i \mu_i}\begin{pmatrix}\sum \alpha_i f_{1i}\\ \sum \alpha_i f_{2i}\end{pmatrix},$$

where α_i is the fraction of atoms of sort A_i. The data on atomic scattering factors can be found in the literature for elements with a nuclear charge from 1 to 92 in the photon energy range 10 eV – 30 keV [18].

Generally speaking, the layer thicknesses l_j are different. Unlike a periodic structure, the combined thicknesses of the pairs of neighbouring layers are not assumed to be constant in depth: $l_1 + l_2 \neq l_3 + l_4 \neq \ldots$. Also different, in general, are the optical paths for the pairs of neighbouring layers: $l_1 n_A + l_2 n_B \neq l_3 n_A + l_4 n_B \neq \ldots$. Moreover, the existence of a structure period is not a priori assumed in any sense.

The reflectivity $R_{s,p}(\lambda, \theta)$ of a multilayer structure for s- and p-polarised radiation incident at an angle θ (the 'direct problem' of multilayer optics) was calculated by the method of recurrent relationships described in the literature [19] and used repeatedly by several authors. The amplitude reflectivity was derived from the system of recurrent relationships

$$r_j = \frac{r_j^F + r_{j+1}\exp(2i\varkappa_{j+1}l_{j+1})}{1 + r_j^F r_{j+1}\exp(2i\varkappa_{j+1}l_{j+1})}, \quad j = 0, \ldots, N, \tag{2}$$

where

$$\varkappa_j = k\left(\varepsilon_j - \sin^2\theta\right)^{1/2}, \quad j = 0, \ldots, N+1; \tag{3}$$

θ is the angle of incidence measured from the normal; $k = 2\pi/\lambda$ is the wave number; and r_j^F is the conventional amplitude reflectivity at the jth interface defined by the Fresnel formulas

$$r_j^F = \frac{\varkappa_j/\eta_j - \varkappa_{j+1}/\eta_{j+1}}{\varkappa_j/\eta_j + \varkappa_{j+1}/\eta_{j+1}}, \quad j = 0, \ldots, N;$$
$$\eta_j = \begin{cases} 1 & \text{for s-polarised radiation,}\\ \varepsilon_j & \text{for p-polarised radiation.}\end{cases} \tag{4}$$

The net reflectivity of the structure (in intensity) is $R = |r_0|^2$. In the calculations set out here, recourse was made to the refined atomic scattering factor files, which are currently available via the Internet [20].

The search for the AMS which satisfies some preassigned criterion best will be referred to as the 'inverse problem' of multilayer optics, or the AMS-optimisation problem. The key step of the optimisation procedure involves the prescription of the goal function F_{gf} for $R(\lambda, \theta_0)$ or $R(\lambda_0, \theta)$ (the subscript implies that the value of an incidence angle or a wavelength is fixed). The goal function was prescribed on some interval of wavelengths or angles and also on several isolated intervals. We introduced a measure of departure of the reflectivity from F_{gf} (the merit function F), which was calculated over the domain of definition of F_{gf} and treated as a function of N independent variables $\{l_j\}$.

The prescription of F_{gf} and the introduction of a norm eventually predetermine the optimisation results. For instance, the simplest formulation of the problem involves the search for an AMS that possesses maximum integral reflectivity $\mathfrak{J}$ over a given interval of wavelengths or photon energies. In this case,

$$F = \mathfrak{J}_\lambda = \int_{\lambda_1}^{\lambda_2} R(\lambda)\,d\lambda \;\text{ or }\; F = \mathfrak{J}_E = \int_{E_1}^{E_2} R(E)\,dE. \tag{5}$$

When determining the AMS whose reflectivity approximates a given function F_{gf} over its domain of definition Λ, the F

function may be taken as

$$F = -\int_{\Lambda} \left[F_{\rm gf} - R(\lambda, \theta_0)\right]^2 \lambda^{-v}\, {\rm d}\lambda\ , \qquad (6)$$

where $v = 0$ or 2.

The 'inverse problem' of multilayer optics cannot be solved by an exhaustive brute-force enumeration. Several attempts of optimising an AMS were reported in the literature [12–15]. In particular, Van Loevezijn et al. [14] employed a version of the Monte-Carlo technique. The use of this technique is limited by the unreliability of solution determination and long computation times (it is well known that a randomly chosen direction is nearly perpendicular to the sought-for one for high space dimensionalities). More sophisticated techniques were also invoked to find the extremum — the method of steepest descent [12, 13] and the simplex method [15].

In our work, the extremum of the function F was determined by the method of steepest descent, which involves the following steps. An initial point $\{l_j^{(0)}\}$ is chosen in the N-dimensional space (the initial structure), and the gradient

$$\nabla F = \left\{\frac{\partial F}{\partial l_j}\right\}, \quad j = 1, ..., N. \qquad (7)$$

is calculated at this point. Next, a small displacement (step) is made along the gradient direction to increase F. The new resultant point serves as the initial one for the step and so on, until the next point finds itself in the vicinity of the maximum. However, difference calculation of the gradient (as calculation of F at simplex points) requires N calculations of the function F. Each of the computation times is also proportional to N. A typically quadratic dependence of the time taken to make a step on the number of layers in the structure under optimisation is evident. Moreover, the number of required steps also increases with N, as a rule. These factors limit the complexity of the problems under solution and the quality of solutions obtained.

To reduce the power of the N-dependence of the computation time, we derived an analytical formula for the partial derivatives of the amplitude reflectivity with respect to layer thicknesses. Differentiation of recurrent relationships (1) gives

$$\frac{\partial r_0}{\partial l_j} = 2{\rm i}\varkappa_j r_j \exp\left(2{\rm i}\sum_{k=1}^{j}\varkappa_k l_k\right) \times \prod_{k=0}^{j-1} \frac{1 - \left(r_k^{\rm F}\right)^2}{\left[1 + r_k^{\rm F} r_{k+1} \exp(2{\rm i}\varkappa_{k+1} l_{k+1})\right]^2}. \qquad (8)$$

The gradient of the function F of the form (5) in the N-dimensional space of the variables $\{l_j\}$ has the form

$$\frac{\partial F}{\partial l_j} = 2{\rm Re}\left[\int_{\lambda_1}^{\lambda_2} \frac{\partial r_0(\lambda)}{\partial l_j}\right] r_0^*(\lambda)\, {\rm d}\lambda\,, \quad j = 1, ..., N\ . \qquad (9)$$

The expressions for the gradient of the merit functions of another type are obtained in a similar way. The use of analytical expressions (8) reduces the N-dependence of the step time to a linear one, resulting in the increase in the computation rate by about a factor of $N/5$. The process convergence was monitored and served as guide for terminating the optimisation. The numerical experiments were controlled via a programme graphic interface. The AMS computation time depended primarily on the number of layers and ranged from several seconds to several hours when using a Pentium 200 Hz PC.

The option of parametric structure optimisation was also provided for. In this case, the layer thicknesses $\{l_j\}$ were treated as analytical functions of several parameters and the discrete variable j.

3. Normal-incidence AMSs with a broad reflection spectrum

We determine the potentialities of an AMS for expanding the reflection band and increasing the integral reflectivity

$$\mathfrak{J}(\lambda_1, \lambda_2) = \int_{\lambda_1}^{\lambda_2} R(\lambda)\, {\rm d}\lambda$$

at normal incidence in the $\lambda > 130$ Å range, where a Mo/Si-based structure is efficient. In the first series of calculations, the domain of definition of $F_{\rm gf}$ was successively expanded from the point $\lambda = 160$ Å to the 130–190 Å interval. The results of this series were compared with a periodic structure optimised in the structure parameters d and γ for maximum reflectivity at $\lambda = 160$ Å (see Table 1, Version 1). The reflectivity of this structure had the shape of an asymmetric bell of width $\Delta\lambda_{1/2} = 9.8$ Å (FWHM).

The aperiodic structure optimised for maximum reflectivity at $\lambda = 160$ Å did not provide any tangible gain in comparison with the periodic structure. Successive extension of the domain of definition of the $F_{\rm gf}$ (Versions 2–4) led to a decrease of the peak reflectivity $R_{\rm max}$ and a wavelength shift of the peak (Fig. 1). In the process, the bell-like shape was gradually abandoned, deep dips appeared in the $R(\lambda)$ profile, and the integral reflectivity in the 120–200 Å interval increased. The AMS optimised for maximum $\mathfrak{J}$ exceeded the periodic one by nearly a factor of two in $\mathfrak{J}$. The like AMSs can be validly used, for instance, in those cases where maximum SXR flux from a broadband source must be formed.

Table 1. Reflection characteristics of the Mo/Si-based AMSs.

Version No.	Figure	$F_{\rm gf}$	$\theta/^\circ$	Domain of definition of $F_{\rm gf}$/Å	$R_{\rm max}$ (%)	$\mathfrak{J}$/Å in the interval		
						130–190 Å	120–200 Å	120–360 Å
1	1,*a*	1.0	0	160	65	7.81	7.99	–
2	1,*b*	1.0	0	152.5–167.5	59	9.75	9.98	–
3	1,*c*	1.0	0	145–175	47	11.64	11.97	–
4	1,*d*	1.0	0	130–190	37	14.77	15.49	–
5	2	0.24	0	130–190	24	13.83	15.72	18.91
6	3	0.16	0	130–300	21	–	11.49	29.46
7	4	0.34	41	130–190	36	19.67	22.92	–

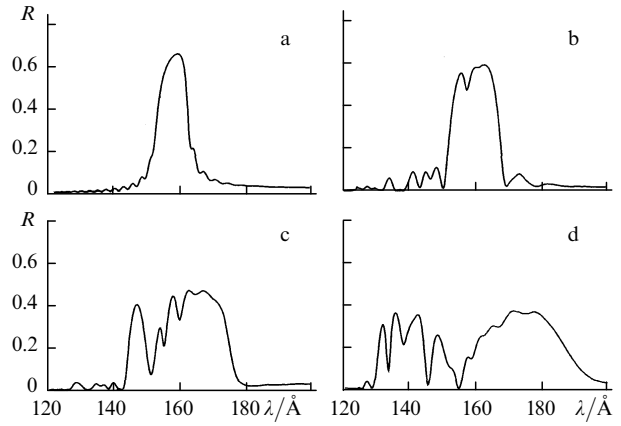

Figure 1. Reflectivities of Mo/Si MMs ($N = 80$) in the 120 – 200 Å interval: the periodic structure optimised in parameters d and γ for maximum $R(\lambda)$ at $\lambda = 160$ Å (a); the AMSs optimised for maximum $\mathfrak{J}$ on the interval 152.5 – 167.5 (b), 145 – 175 (c), and 130 – 190 Å (d).

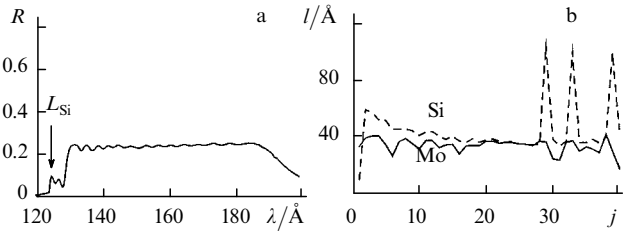

Figure 2. Reflectivity (a) and layer thicknesses (b) of the AMS (Mo/Si, $N = 80$) optimised for minimum departure of R from the level 0.24 in the 130 – 190 Å interval (Table 1, Version 5).

The existence of dips in the $R(\lambda)$ profile in Version 4 makes this structure unsuitable for some applications (e.g., for recording line spectra). Therefore, in the subsequent calculations, our intention was to find structures with a constant magnitude of $R(\lambda)$. To this end, the goal function F_{gf} was reduced to such a level that the area beneath it was equal to the corresponding value of $\mathfrak{J}$ attained in the previous series of calculations. Moreover, F was changed so as to make strong excursions of the $R(\lambda)$ curve from F_{gf} disadvantageous [by using quadratic norm (6)]. When F_{gf} was preassigned at the level of 0.24 on the 130 – 190 Å interval, we succeeded in deriving an AMS with a nearly constant reflectivity (Table 1, Version 5; Fig. 2). Note that this structure is nearly equal to that of Version 4 in integral reflectivity on the 130 – 190 Å interval; in the 120 – 200Å interval, it is even superior to that of Version 4 in $\mathfrak{J}$. This MM can fulfil the function of focusing radiation in a diffraction spectrometer with an operating range of about 60 Å in width. The existence of the L-edge of absorption in Si (indicated by the L_{Si} arrow in Fig. 2) lowers the efficiency of Mo/Si-based MMs in the $\lambda < 125$ Å range and makes it impossible to extend the operating range towards shorter wavelengths.

Similar results are also obtained in the 130 – 300 Å interval (Table 1, Version 6; Fig. 3). In this case it was possible to find an AMS with an average reflectivity of about 15% and an integral reflectivity $\mathfrak{J}$ (130 – 300 Å) = 25.4 Å.

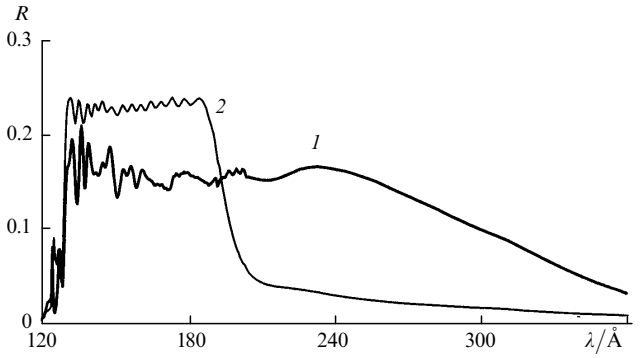

Figure 3. Reflectivity of the AMS (Mo/Si, $N = 80$) optimised for minimum departure of R from the level 0.16 in the 130 – 300 Å interval (Table 1, Version 6; 1) and of the AMS derived in Version 5 (2).

4. Broadband AMS-based polarisers

Multilayer structures with a broad reflection spectrum prove to be broadband polarisers as well. The issue of polarisance of periodic Mo/Si MMs in the $\lambda \sim 170$ Å range was studied theoretically and experimentally [5, 6, 21, 22]. For the above MMs, the peak of the polarisance, defined as $P = (R_s - R_p) \times (R_s + R_p)^{-1}$, was attained near the incidence angle $\theta \approx 41^\circ$. Wavelength tuning is effected by changing the angle of incidence and is attained at the expense of a lowering of the polarisance, which limits the tunabilty range.

The use of two successive reflections from two similar MMs somewhat extends the operating range but results in a reduction of the net reflectivity. Here, we propose a new type of an x-ray optical element — a polariser which ensures a high polarisance for a fixed angle of incidence in a rather broad wavelength range. Fig. 4 shows the polarisance $P(\lambda)$ and the reflectivity for s-polarised radiation $R_s(\lambda)$ for three AMSs optimised for uniform reflectivity in the ranges 88 – 124 Å (Rh/B_4C, $\theta = 42.5^\circ$), 130 – 190 Å (Mo/Si, $\theta = 41^\circ$), and 190 – 300 Å ($MoSi_2/Si$, $\theta = 41.5^\circ$). One can see that $P(\lambda)$ of the Mo/Si-based polariser varies from unity to 0.94 in the entire operating range (130 – 190 Å) and decreases to 0.88 towards $\lambda = 200$ Å. Both in reflectivity and the width of the operating range, this single-mirror polariser is superior

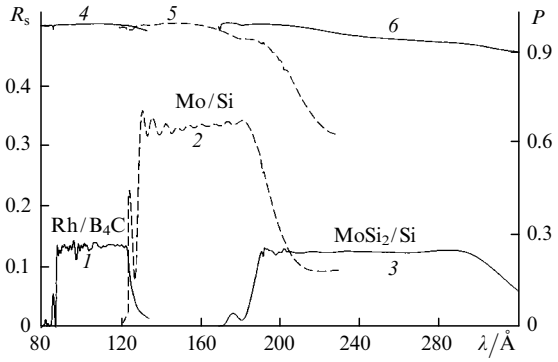

Figure 4. Reflectivity for s-polarised radiation (1 – 3) and polarisance (4 – 6) of the three AMSs optimised for uniform reflection in the ranges 88 – 124 Å (Rh/B_4C, $\theta \approx 42.5^\circ$, $N = 120$; **1, 4**), 130 – 190 Å (Mo/Si, $\theta \approx 41^\circ$, $N = 40$; **2, 5**), and 190 – 300 Å ($MoSi_2/Si$, $\theta \approx 41.5^\circ$, $N = 20$; **3, 6**). The MM polariser for the 130 – 190 Å range corresponds to Version 7 of Table 1.

to the two-mirror polariser of Ref. [22] intended for the same range.

Reasonably good results in the shorter wavelength range are furnished by the Rh/B_4C pair ($F_{gf} = 0.14$) and in the longer wavelength range by the $MoSi_2/Si$ pair ($F_{gf} = 0.124$). As with broadband normal-incidence MMs, an increase in reflectivity can be attained only by sacrificing the width of the operating range.

5. Multilayer structures with isolated reflection maxima

In some special cases, there is a demand for MMs that simultaneously select several wavelength intervals rather than one. For instance, in the spectroscopic studies of elementary processes involving multiply charged ions and in plasma diagnostics, the intensities and the spectral shapes of the Balmer series lines of ion C vi with wavelengths $\lambda = 182$ Å (the $3 \rightarrow 2$ transition, the H_α line) and 135 Å ($4 \rightarrow 2$, H_β) are of particular interest. To determine the AMS possessing the relevant reflectivity, the F_{gf} function was defined at the two points: $\lambda_1 = 135$ and $\lambda_2 = 182$ Å.

The wavelength dependence of the reflectivity of the AMS obtained in this case is plotted in Fig. 5. The respective peak reflectivities are 61% and 43% against 74% and 53% for the two different periodic structures optimised for maximum reflectivities at λ_1 and λ_2. The integral reflectivity of the resultant AMS is 10.3 Å, which exceeds those of the periodic ones by, respectively, the factors of 1.77 and 1.20.

6. Optimisation of a Mo/Si structure for maximising peak reflectivity

As mentioned above, defining F_{gf} at only one point makes it possible to optimise an AMS as regards to its peak reflectivity. It turned out that the AMS optimised for peak reflectivity at $\lambda = 160$ Å was only insignificantly (by 0.05 %) superior to the periodic one optimised in the γ and d parameters to attain maximum reflectivity at this wavelength. In the $\lambda > 200$ Å range, the AMSs were capable of furnishing a substantial gain. This effect is accomplished primarily by varying the thickness of only one (upper) layer. At $\lambda = 300$ Å, for instance, the peak reflectivity of the optimum AMS was 1.3 times that of the periodic one. In this case, it is possible to restrict ourselves to a significantly smaller number of layers (Fig. 6).

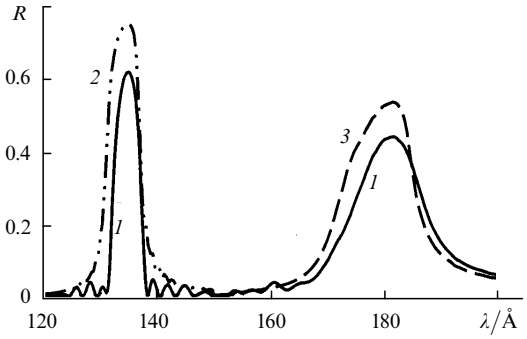

Figure 5. Reflectivity of the AMS (Mo/Si, $N = 80$) optimised for maximum sum $R(\lambda_1) + R(\lambda_2)$, where $\lambda_1 = 135$ Å and $\lambda_2 = 182$ Å **(1)**, and of the two periodic mirrors optimised for maximum $R(\lambda_1)$ (2) or $R(\lambda_2)$ (3).

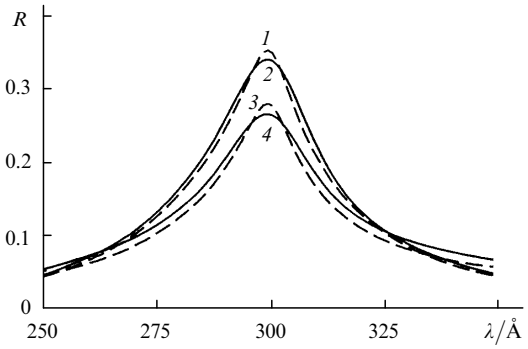

Figure 6. Reflectivities of the Mo/Si-based AMSs (1, **2**) and the periodic MMs (3, **4**) optimised for maximum reflectivity at $\lambda = 300$ Å for $N = 50$ (1, **3**) and 20 (2, **4**).

7. Grazing-incidence AMSs for the hard x-ray range

From the standpoint of multilayer optics design, the hard x-ray range has several specific features caused by the relative smallness of δ and β. Here, the high efficiency of multilayer optics is attained by using small (grazing) angles of incidence. (These angles are nevertheless much higher than those which provide 'total external reflection' from a thick layer of the material in the same spectral region.) The second feature is that the requisite number of layers increases markedly in many cases.

The capabilities of the technique for optimising AMSs for the hard x-ray range will be demonstrated by the example of the following problem. It is necessary to calculate AMSs, made of different pairs of materials, which possess maximum uniform reflectivity in the 15–25 keV range. An AMS obtained by parametric optimisation served as the initial approximation. To this end, the simplex method was employed to search for the maximum of precisely the same merit function which was intended for use in global optimisation. In the parametric optimisation, the dimensionality of space was equal to the number of parameters and was far less than the number of layers. A seven-parameter model ($A_{1,2}$, $t_{1,2}$, d_0, γ_0 and α) was profitably employed in the solution of this problem:

$$l_j = \gamma_j\left[d_0 + A_1 \exp(-Z_j/t_1) + A_2 \exp(-Z_j/t_2)\right], \quad j = 1, \ldots, M,$$

$$\gamma_j = \begin{cases} \gamma_0 + \alpha Z_j, & \text{even } j, \\ 1 - \gamma_0 - \alpha Z_j, & \text{odd } j, \end{cases} \qquad (10)$$

$$Z_j = \sum_{k=1}^{j} l_k.$$

Employing the structures, derived in model (10), as the initial approximation resulted in a considerable reduction of the time required for global optimisation, when the thicknesses of all layers were treated as independent variables.

Fig. 7 shows the reflection spectrum of an AMS based on the Ni/C pair (number of layers $N = 800$, grazing angle of 0.01 rad). The goal function was prescribed as the plato $F_{gf} = R_0(E) = 0.22$ on the 15–25 keV (0.496–0.827 Å)

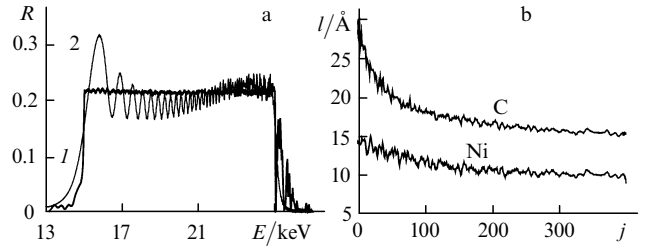

Figure 7. Reflectivity (a) and layer thicknesses (b) of the AMS (Ni/C, $N = 800$, grazing angle of 0.01 rad) optimised for minimum departure of R from the level 0.22 in the 15 – 25 keV interval: (1) global optimisation; (2) parametric optimisation in the context of model (10), which served as the initial approximation for the global optimisation.

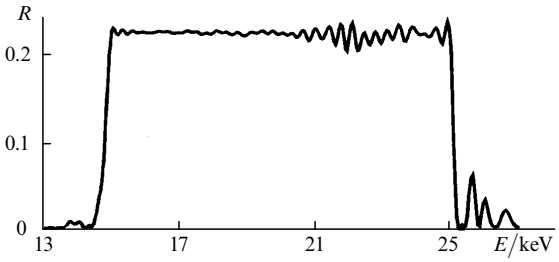

Figure 8. Reflectivity of the AMS (Os/C, $N = 140$, 0.01 rad) optimised for minimum departure of R from the level 0.24 in the 15 – 25 keV interval.

interval. Shown in Fig. 8 is the reflection spectrum of an Os/C AMS ($N = 140$, 0.01 rad). The goal function was prescribed as the plato $F_{gf} = R_0(E) = 0.24$ on the same interval. As regards integral reflectivity ($\mathfrak{I}_E = 2.17$ and 2.25 keV), the structures derived are considerably superior to any periodic MMs of the same range. For instance, a periodic MM (Os/C, $N = 200$, 0.01 rad) optimised for maximum reflectivity at $E_0 = 20$ keV affords $R(E_0) = 0.92$ and $\mathfrak{I}_E = 0.66$ eV. A periodic Os/C MM optimised for maximum $\mathfrak{I}_E$ in the 15 – 25 keV interval offers $\mathfrak{I}_E = 1.09$ eV. In this case, the reflectivity peak shifts to $E_0 = 16.8$ keV and $R(E_0) = 0.78$.

8. On the required accuracy of reproducing the layer thicknesses

The reflectivities of periodic MMs measured experimentally are known to be somewhat below the calculated ones. This is due to the existence of substrate and interlayer roughness, the formation of transition layers, the departures of actual layer densities from the tabulated values, and some other reasons. One of these reasons is an imperfect reproducibility of the layer thicknesses during the MM deposition process. We compared the stability of the calculated $R(\lambda)$ functions for periodic and aperiodic MMs with respect to randomisation of the layer thicknesses: $l_j = l_j^{(0)} + \delta l_j$, where δl_j is a random number with an r.m.s. value σ.

A periodic structure with reflectivity peak at $\lambda = 135$ Å and an aperiodic structure with a uniform reflection in the 130 – 190 Å range were compared. It turned out that the plot of $R(\lambda)$ experienced a substantial deformation beginning with $\sigma \sim 3 - 4$ Å (in either case, the shape and the depth of the deformations depend on a particular realisation of the set $\{\delta l_j\}$ of random numbers). We therefore believe that the synthesis of aperiodic MMs imposes the same requirements on the reproducibility of layer thicknesses as the synthesis of periodic ones.

9. Conclusions

A numerical technique was developed for determining multilayer structures possessing a given reflection spectrum or optimised as regards to other functional criteria. A search was made for structures with maximum integral reflectivity or with maximum uniform reflectivity over a given wavelength interval, structures with a high polarisance, those with several reflection maxima, etc. It was determined that the multitude of realisations of a Mo/Si-based AMS contains structures exceeding the regular one in width of the operating range, integral reflectivity, and peak reflectivity.

The search yielded AMSs with a constant normal-incidence reflectivity in the 130 – 190 Å (24%) and 130 – 300 Å (15%) ranges and AMSs with a high polarisance and a nearly constant R throughout the 88 – 124, 130 – 190, and 190 – 300 Å intervals at oblique incidence at a fixed angle $\theta \sim 41 - 43^\circ$. AMSs with several isolated reflection maxima which are not Bragg orders of each other were calculated. A Mo/Si-based mirror was calculated whose reflectivity at $\lambda = 300$ Å exceeded that of the optimum periodic structure by one third. The aperiodic multilayer mirrors are intended for control of the parameters (divergence, polarisation, spectral composition) of SXR radiation beams and development of broadband stigmatic optical/spectroscopic instruments with a high angular and spectral resolution.

Acknowledgements. The authors thank I L Beĭgman and N N Salashchenko for helpful discussions. This work was supported by the Russian Foundation for Basic Research (Project No. 00-02-17717) and the 'Integration' Federal Dedicated Programme (Project No. 2.1-35).

References

1. Spiller E Appl. Opt. **15** 2333 (1976)
2. Vinogradov A V, Zel'dovich B Ya Opt. Spektrosk. **42** 709 (1977)
3. Joensen K D, Gorenstein P, Wood J, Christensen F E, Hoghoj P Proc. SPIE Int. Soc. Opt. Eng. **2279** 180 (1994)
4. Da Silva L B, Barbee T W Jr., Cauble P, et al. X-Ray Lasers 1996 (Proceedings of the Fifth International Conference on X-Ray Lasers, Lund, Sweden, 1996) S Svanberg, C-G Wahlstrom (Eds) (Bristol: IOP Publishing, 1996) p. 496
5. Yanagihara M, Maehara T, Nomura H, Yamamoto M, Namioka T Rev. Sci. Instrum. **63** 1516 (1992)
6. Ragozin E N, Kolachevsky N N, Mitropolsky M M, Pokrovsky Yu Yu, Shevelko A P, Vasil'ev A A, Platonov Yu Ya, Salashchenko N N Proc. SPIE Int. Soc. Opt. Eng. **2520** 309 (1995)
7. Andreev S S, Gaponov S V, Salashchenko N N, et al. Proc. SPIE Int. Soc. Opt. Eng. **3406** 45 (1998)
8. Ragozin E N, Kolachevsky N N, Mitropolsky N N, Fedorenko A I, Kondratenko V V, Yulin S A Phys. Scr. **47** 495 (1993)
9. Beĭgman I L, Pokrovskiĭ Yu Yu, Ragozin E N Zh. Eksp. Teor. Fiz. **110** 1783 (1996) [J. Exp. Theor. Phys. **83** 981 (1996)]
10. Sobel'man I I, Zhitnik I A, Ignat'ev A P, et al. Pis'ma Astron. Zh. **22** 605 (1996)
11. Andreev S S, Kolachevskiĭ N N, Pirozhkov A S, Ragozin E N, Salashchenko N N Kratk. Soobshch. Fiz. (3) **32** (1998) [Bull. Lebedev Phys. Inst. (3) **27** (1998)]
12. Meekins J F, Cruddace R G, Gursky H Appl. Opt. **26** 990 (1987)
13. Vernon S P, Stearns D G, Rosen R S Opt. Lett. **18** 672 (1993)
14. Van Loevezijn P, Schlatmann R, Verhoeven J, van Tiggelen B A, Gullikson E M Appl. Opt. **35** 3614 (1996)

15. Joensen K D. Proc. SPIE Int. Soc. Opt. Eng. **3113** 500 (1997)
16. Balakireva L L, Kozhevnikov I V J. X-Ray Sci. Technol. **6** 150 (1996)
17. Kozhevnikov I V, Bukreeva I N, Ziegler E Proc. SPIE Int. Soc. Opt. Eng. **3448** 322 (1998)
18. Henke B L, Gullikson E M, Davis J C At. Data Nucl. Data Tables **54** 835 (1993)
19. Vinogradov A V, Brytov I A, Grudskiĭ A Ya, et al. Zerkal'naya Rentgenovskaya Optika (X-Ray Mirror Optics) (Leningrad: Mashinostroenie, 1989)
20. Soufli R, Gullikson E M Proc. SPIE Int. Soc. Opt. Eng. **3113** 222 (1997); ⟨http://cindy.lbl.gov/optical_constants/⟩.
21. Vasil'ev A A, Mitropol'skiĭ M M, Platonov Yu Ya, Pokrovskiĭ Yu Yu, Ragozin E N, Salashchenko N N, Shchevel'ko A P Kvantovaya Elektron. (Moscow) **22** 408 (1995) [Quantum Electron. **25** 387 (1995)]
22. Kolachevskiĭ N N, Pirozhkov A S, Ragozin E N Kvantovaya Elektron. (Moscow) **25** 843 (1998) [Quantum Electron. **28** 821 (1998)]